Refractive index profiles and propagation losses in bent optical fibers

Pauli Kiiveri,* **Mikko Kuusisto, Joona Koponen, Ossi Kimmelma, Ville Aallos, Juha Harra, Hannu Husu, and Päivi Kyllönen**
nLIGHT Inc., Lohja, Finland

Abstract. A better understanding of stress effects that affect the bending losses in active and passive optical fibers allows us to improve fiber system designs and helps to optimize refractive index profiles in high power, large mode area laser fibers. Bending an optical fiber affects the light in a fiber core by two different phenomena. First, the curved shape of the waveguide changes the light propagation. The second phenomenon is the refractive index change caused by the mechanical stress in a bent optical fiber. The refractive index changes due to bending stresses are estimated by the elasto-optic and stress-optic models. The light propagation in a curved waveguide can be modeled by applying the electromagnetic wave theory together with the conformally transformed refractive index profiles that include the stress effects. The modeled refractive index profiles that include the bending stress-induced index changes are compared with the refractive index profiles that were measured from actual bent optical fibers. We tested if this comparison would allow us to estimate stress-optic coefficient C_2 values in stress-optic model. Measured bend loss values are compared to the bend loss values simulated with the modeled refractive index profiles. © *The Authors. Published by SPIE under a Creative Commons Attribution 4.0 International License. Distribution or reproduction of this work in whole or in part requires full attribution of the original publication, including its DOI.* [DOI: 10.1117/1.OE.61.12.126106]

Keywords: bent optical fiber; refractive index; bending stress; elasto-optic; stress-optic; modeling; bending loss.

Paper 20220889G received Aug. 10, 2022; accepted for publication Nov. 28, 2022; published online Dec. 22, 2022.

1 Introduction

Bending stress-induced refractive index changes are estimated using the elasto-optic and stress-optic models. The refractive index profiles are calculated with both models. To improve the index profile estimations, we will use mixed elastic modulus values for doped waveguide glass.

A virtual refractive index profile that simulates a curved waveguide can be calculated using conformal transformation. The conformal transformation can be applied also to a refractive index profile of a waveguide already containing the bending stress-induced refractive index change. The conformally transformed refractive index profile can be used for simulating the bending losses of optical modes in a bent optical fiber.

2 Conformal Transformation of Refractive Index Profiles

In this article, a curved waveguide refers to an unstressed curved waveguide and a bent fiber refers to a bent waveguide with stress effects. A curved fiber can be represented by a radius of curvature and by the refractive index profile $n(x)$ of the waveguide, where x is a radial coordinate in the fiber core.

Conformal transformation is a coordinate transformation that preserves the angles. Most models of curved dielectric waveguides apply conformal transformation, where the index profile of a curved waveguide is transformed into a modified index profile in a straight waveguide. So, the effect of curving, affecting the light, is simulated by a modified index profile of a waveguide.

*Address all correspondence to Pauli Kiiveri, pauli.kiiveri@nLight.net

The conformal transformation (of an index profile) that models the curvature effect of a waveguide, is based on locally invertible complex analytic functions.[1,2]

Conformal transformation (conformal mapping) is a general method that can be used, e.g., for transforming a curved waveguide to a straight waveguide, where simpler simulation algorithms can be used to study the properties of the waveguide. The conformal transformation is based on the mathematical properties of complex plane. The transformation itself is an exact, not an approximative method, so the solutions of Maxwell's equations in a non-transformed waveguide and in a transformed waveguide are equal.

We need a coordinate transformation between the coordinates (x, y) in a curved physical waveguide, where the radial coordinate $r = \sqrt{x^2 + y^2}$ is given relative to the center of the curvature in a curved waveguide and coordinates (x', y') that are given relative to the center of the waveguide in a virtual straight waveguide, see Fig. 1. When a waveguide, like an optical fiber, has a circular symmetry, the applied conformal coordinate transformation between the coordinate x' in a straight fiber and the radial coordinate r in a curved fiber is

$$x' = R \ln\left(\frac{r}{R}\right), \tag{1}$$

where x is a coordinate in a curved waveguide system, where $x = y = 0$ in the center of the curvature. $r = \sqrt{x^2 + y^2}$ is a radial coordinate in the curved waveguide relative to the center of curvature, (notice, if $y = 0$ then $r = x$). R is a distance between the center of the curvature and the center of the waveguide, i.e., radius of curvature. x', y' are coordinates in a straight waveguide with $\mathrm{x}' = 0$ in the center of the waveguide.

If $r \sim R$, then Taylor approximation of the x' in Eq. (1) is

$$x' \approx r - R.$$

Radial coordinate r in the curved waveguide can be solved from Eq. (1), where $r = 0$ at the center of the curvature.

$$r = \mathrm{Re}^{\frac{x'}{R}}. \tag{2}$$

The original refractive index profile $n(r)$ of a curved physical waveguide is conformally transformed as a modified index profile $n_c(x')$ in a virtual straight waveguide. The transformed index profile $n_c(x')$ is given by a product[1,3]

$$n_c(x', R) = \left|\frac{\mathrm{du}}{\mathrm{dw}}\right| \cdot n(r), \tag{3}$$

where the complex variables are $u = x + iy$ and $w = x' + iy'$.

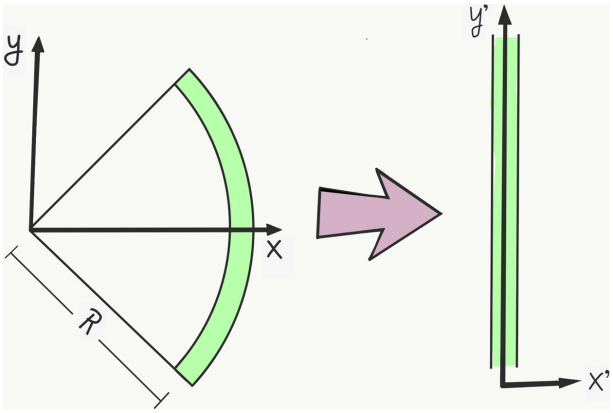

Fig. 1 A coordinate x in a curved waveguide and a related coordinatex' in a straight waveguide.[1,2]

Because of the rotation symmetry of the curved waveguide system, we can study the curved and straight waveguides at the positions where $y = 0$ and $y' = 0$. Then the values of the complex variables are $u = x = r$ and $w = x'$. Thus, using Eq. (3) and coordinate transformation in Eq. (2)

$$|\mathrm{d}u/\mathrm{d}w| = \mathrm{d}x/\mathrm{d}x' = \mathrm{d}r/\mathrm{d}x' = e^{x'/R}.$$

The conformal transformation $n_c(x')$, in Eq. (3), of the original refractive index profile $n(r)$, is

$$n_c(x', R) = e^{\frac{x'}{R}} \cdot n(r). \tag{4}$$

Equation (4) gives a virtual index profile $n_C(x', R)$ in a straight waveguide that simulates the curving of a waveguide. An index profile $n_c(x', R)$ is a conformal transformation of the original refractive index profile $n(x)$ of a waveguide without stresses

$$n_C(x', R) = e^{\frac{x'}{R}} n(x) \approx \left(1 + \frac{x'}{R}\right) n(x), \tag{5}$$

where $n(x)$ is the original refractive index profile of a waveguide and $x' = R\ln(\frac{r}{R}) \approx r - R$, when $r \sim R$. We can use a Taylor approximation $(1 + \frac{x'}{R})$ in Eq. (5), if $\frac{x'}{R} \ll 1$.

The light transmission in a curved waveguide is simulated (e.g., with a semivectorial beam propagation method) using a conformal mapping of the original refractive index profile $n(x)$ of the waveguide. The transformed profile $n_c(x', R)$ is given in Eq. (5), with the coordinate $x' = 0$ at the center of the waveguide. After conformal transformation, e.g., an originally constant refractive index profile $n(x)$ in a bent waveguide will increase on the outer side and decrease on the inner side of the transformed waveguide as shown in Fig. 2.

Conformal transformation of a bent, cylinder symmetric optical fiber allows to use simple methods of solving the Maxwell equations. The results, including bending stresses in the input, should be similar as would be found, e.g., by applying the finite-element method (FEM)[4] for the same fiber. When using the cylinder symmetry of the system and conformal transformation, one can simplify and speed up the waveguide simulations without losing accuracy.

2.1 *Conformal Transformation of Bending Stress Induced Refractive Index Profiles*

Bending induces tensile stress on the outer side and compressive stress on the inner side of a bent fiber. Stress-induced refractive index changes have opposite sign compared with the virtual index changes due to curving of the waveguide.

We can use the elasto-optic (EO) or the stress-optic (SO) model to estimate the radial index profile change due to bending-induced stresses. The selection between the two models depends on the available material parameter data for the optical fibers. If the same material parameter data

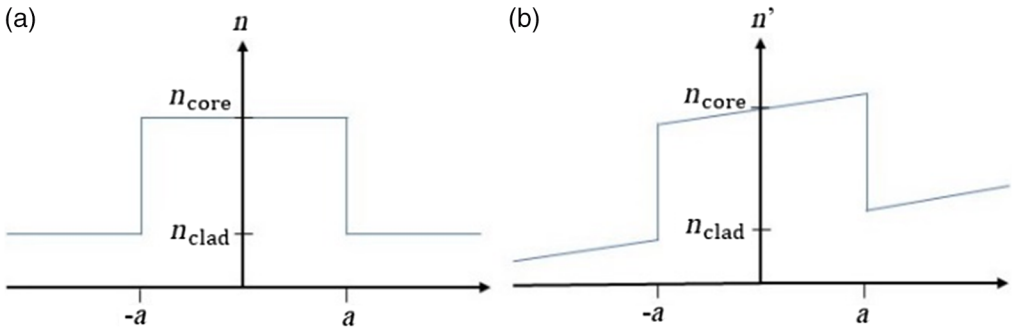

Fig. 2 (a) A step index refractive index profile and (b) the effect of conformal transformation.

will be converted from one model to the other, the calculated refractive index changes will be identical in both models.

3 Elasto-optic Model for Bending Stress Induced Refractive Index Changes

3.1 *Bending Stress Induced Refractive Index Changes*

Let us study a circular waveguide having an originally unstressed radial refractive index profile $n(x)$. The bending stress induced elasto-optic (EO) refractive index change $\Delta n_{\mathrm{EO}}(x,\lambda,R)$ in that waveguide is[2]

$$\Delta n_{\mathrm{EO}}(x,\lambda,R) = -\frac{n_{\mathrm{SiO2}}^2(\lambda)}{2}[p_{12} - v(p_{11}+p_{12})]\left(\frac{x}{R}\right)n(x,\lambda), \tag{6}$$

where p_{11} is an elasto-optic Pockels' coefficient, p_{12} is an elasto-optic Pockels' coefficient, $n(x,\lambda)$ is the unstressed index profile of the waveguide. The value $n(x,\lambda)$ varies as a function of the radial position in the fiber. $\Delta n_{\mathrm{EO}}(x,\lambda,R)$ is the stress-induced index change in the elasto-optic model, $n_{\mathrm{SiO2}}(\lambda)$ is the refractive index of undoped and unstressed SiO_2 at the applied wavelength λ. x is the radial coordinate in the waveguide with $x = 0$ in the center of the waveguide. R is the bending radius of the waveguide.

Some elasto-optic coefficients are listed in Table 1. Slightly different sets of Poisson's ratio (ν) and elastic modulus (E) values for fused silica are given in the references.[5–8] We will use the values given in Ref. 5 for SiO_2.

A coefficient k is defined in Eq. (7). It is used only to shorten the equations where it will be applied. Using the values of EO-coefficients p_{11}, p_{12}, and Poisson's ratio ν for SiO_2 given in Table 1, the value of the coefficient k in SiO_2 glass at $\lambda = 630$ nm is

$$k = -\frac{n_{\mathrm{SiO2}}^2(\lambda)}{2}[p_{12} - v(p_{11}+p_{12})] = -0.21858. \tag{7}$$

The bending stress-induced index profile $n_{\mathrm{EO}}(x)$, Eq. (8), in the elasto-optic stress model,[2] is a sum of the original unstressed profile $n(x,\lambda)$ and stress-induced index change $\Delta n_{\mathrm{EO}}(x,\lambda,R)$ given in Eq. (6):

$$\begin{aligned} n_{\mathrm{EO}}(x,\lambda,R) &= n(x,\lambda) + \Delta n_{\mathrm{EO}}(x,\lambda,R) \\ &= n(x,\lambda) - \frac{n_{\mathrm{SiO2}}^2(\lambda)}{2}[p_{12} - v(p_{11}+p_{12})]\left(\frac{x}{R}\right)n(x,\lambda) \\ &= n(x,\lambda) + k\left(\frac{x}{R}\right)n(x,\lambda), \end{aligned} \tag{8}$$

where $n(x,\lambda)$ is the refractive index profile of an unstressed straight waveguide.

The index profile $n_{\mathrm{EO}}(x,\lambda)$ in Eq. (8) does not yet include the conformal transformation that will be needed to model the curvature effect.

Table 1 Elasto-optic (EO) coefficients in the Handbook of Optics 1995, Table 17.[5]

$p_{11} = 0.121$	at 630 nm
$p_{12} = 0.270$	at 630 nm
$v = 0.164$	
$E_{\mathrm{SiO_2}} = 72.6$ GPa	

The refractive index of SiO_2 is $n = 1.4572$ at 630 nm.[9] The refractive index $n(\lambda)$ at other wavelengths can be calculated using the Sellmeier equation. [10,11]

We can calculate the refractive index profile of a bent waveguide including the elasto-optic effect. The stress-induced index change $\Delta n_{EO}(x, \lambda, R)$ in Eq. (6), becomes as

$$\Delta n_{EO}(x, \lambda, R) = k\left(\frac{x}{R}\right) n(x, \lambda). \tag{9}$$

The refractive index profile with bending stress-induced index change, but without conformal transformation, is

$$n_{EO}(x, \lambda, R) = n(x, \lambda) + \Delta n_{EO}(x, \lambda, R).$$

Using the $\Delta n_{EO}(x, \lambda, R)$ value in Eq. (9), the stress induced refractive index profile becomes as

$$n_{EO}(x, \lambda, R) = \left(1 + k\left(\frac{x}{R}\right)\right) n(x, \lambda). \tag{10}$$

The two effects, unstressed curving of a waveguide and bending induced stresses modify the refractive index profile to opposite directions: curving moves the electromagnetic field to the direction away from the center of the curvature. So, it virtually increases refractive index at the outer edge of the core. The bending induced stresses increase the refractive index value in the core in inner side of the curvature and decrease the refractive index at the outer side of the curvature, see Fig. 3. When combined, these two phenomena will have opposite effects on the refractive index profile.

The stress-induced index change $\Delta n_{EO}(x, \lambda, R)$ in Eq. (9) has an opposite sign (since k is negative) compared to the virtual index change $(\frac{x'}{R})n(x)$ caused by curving of the waveguide. This (curvature related) virtual index profile was calculated using the conformal transformation $n_C(x, \lambda, R) = (1 + \frac{x}{R})n(x, \lambda)$ in Eq. (5). The size of the bending stress-induced index change is about 22% of the curving related transformation effect of the same waveguide. The stress-induced index change partly compensates for the virtual refractive index change due to curving of the waveguide, see Eq. (15).

3.2 *Conformal Transformation of Elasto-optic Refractive Index Profiles*

All the refractive index values are wavelength dependent even when we do not have written it explicitly in the following equations. We will apply the conformal transformation of a curved waveguide, given in Eq. (5), to the bending stress-induced elasto-optic refractive index profile

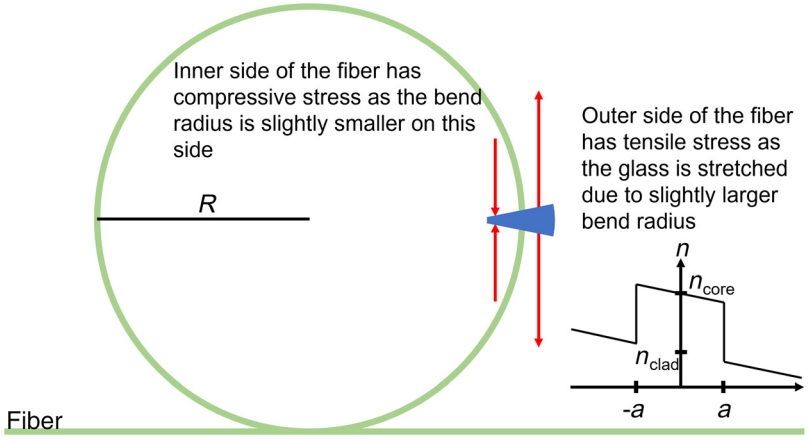

Fig. 3 Stresses and the stress-induced index profile in a bent optical fiber.

$n_{EO}(x, \lambda, R)$ in Eq. (10). This gives us the virtual, conformally transformed refractive index profile $n_{CEO}(x, R)$ in a bent waveguide containing stresses

$$n_{CEO}(x, R) = \left(1 + \frac{x}{R}\right) n_{EO}(x) = \left(1 + \frac{x}{R}\right)[n(x) + \Delta n_{EO}(x, R)], \tag{11}$$

where $n(x)$ is a refractive index profile of a straight fiber and $\Delta n_{EO}(x, R)$ is the refractive index change due to bending induced stresses.

Inserting the $\Delta n_{EO}(x)$ from Eq. (6) into Eq. (11), we have the conformally transformed index profile of a bent fiber

$$n_{CEO}(x, R) = \left(1 + \frac{x}{R}\right)\left[n(x) - \frac{n_{SiO2}^2}{2}(p_{12} - v(p_{11} + p_{12}))\left(\frac{x}{R}\right)n(x)\right]. \tag{12}$$

Using the coefficient k defined in Eq. (7), this is

$$\begin{aligned} n_{CEO}(x, R) &= \left(1 + \frac{x}{R}\right)\left[n(x) + k\left(\frac{x}{R}\right)n(x)\right] \\ &= n(x) + k\left(\frac{x}{R}\right)n(x) + \left(\frac{x}{R}\right)n(x) + k\left(\frac{x}{R}\right)^2 n(x). \end{aligned} \tag{13}$$

We can remove the small, second-order term $k(\frac{x}{R})^2 n(x)$. Then the refractive index profile $n_{EO}(x, R)$, including curving and stress effects, is

$$n_{CEO}(x, R) = \left[1 + (1 + k)\left(\frac{x}{R}\right)\right] n(x), \tag{14}$$

where $n(x)$ is the original refractive index profile of a straight fiber, and k is defined in Eq. (7).

Equation (14) gives the virtual refractive index profile $n_{CEO}(x, R)$ of a curved waveguide with bending stress. In Eq. (14), we can identify the combined refractive index change $\Delta n_{CEO}(x, R)$ due to the curvature and stresses

$$\Delta n_{CEO}(x, R) = (1 + k)\left(\frac{x}{R}\right) n(x). \tag{15}$$

Applying the refractive index value $n = 1.4572$ of SiO_2 at 630 nm in Eq. (7) and using Eq. (14) gives the virtual refractive index $n_{CEO}(x, R)$ of a curved SiO_2 waveguide including stresses

$$\begin{aligned} n_{CEO}(x, R) &= n(x) + \Delta n_{CEO}(x, R) \\ &= \left(1 + 0.7838\left(\frac{x}{R}\right)\right) n(x). \end{aligned} \tag{16}$$

Equation (16) is a conformal transformation of a refractive index profile of a bent silica fiber including stresses by the elasto-optic model. Equation (16) is based on the SiO_2 material parameters and is thus missing dopant material effects.

3.3 *Effective Bending Radius in the Elasto-optic Model*

Using the $n_{CEO}(x, R)$ in Eq. (12) and the elasto-optic coefficients p_{11} and p_{12}, we can define an equivalent bending radius R_{eff}, which includes the curving and stress effects, similarly as has been done in Ref. 2. Effective bending radius includes a multiplier for the real bending radius R of the fiber. The multiplier is a short way to indicate how much the material dependent stress effects change the refractive index of a bent optical fiber. Using Eqs. (5) and (12) we can write

$$n_{\mathrm{CEO}}(x, R_{\mathrm{eff}}) = \left(1 + \frac{x}{R_{\mathrm{eff}}}\right) n(x)$$
$$= \left(1 + \frac{x}{R}\right)\left[1 - \frac{n^2}{2}[p_{12} - v(p_{11} + p_{12})]\left(\frac{x}{R}\right)\right] n(x). \tag{17}$$

Solving R_{eff} from Eq. (17) and removing the small second-order terms $(\frac{x}{R})^2$ the effective bending radius is

$$R_{\mathrm{eff}} = \frac{R}{\left[1 - \frac{n^2}{2}(p_{12} - v(p_{11} + p_{12}))\right]}. \tag{18}$$

Substituting the elasto-optic p_{11} and p_{12} values of undoped silica, given in Table 1, into Eq. (18), and using the refractive index value $n = 1.4572$ (SiO_2 at 630 nm), the effective bending radius in Eq. (18) is

$$R_{\mathrm{eff}} = 1.280R. \tag{19}$$

This is the effective bending radius of a pure SiO_2 waveguide. The effective bending radius, $R_{\mathrm{eff}} = 1.280R$, is derived using conformal mapping and stress-induced index change in the elasto-optic model.

Using the effective bending radius $R_{\mathrm{eff}} = 1.280R$ of a SiO_2 waveguide, the conformally transformed elasto-optic model (CEO) in Eq. (16) can be written with an expression similar to the conformal mapping in Eq. (5)

$$n_{\mathrm{CEO}}(x, R) = \left(1 + \frac{x}{R_{\mathrm{eff}}}\right) n(x) = \left(1 + \frac{x}{1.280R}\right) n(x). \tag{20}$$

The $n_{\mathrm{CEO}}(x)$in Eq. (20) is the virtual refractive index profile of a bent optical fiber including the elasto-optic stress effect. It can be used in the fiber simulations if doping effects can be neglected.

4 Stress-optic Model for Bending Stress Induced Refractive Index Changes

Alternatively, the stress induced refractive index change can be calculated also using the stress-optic (SO) model[9] instead of the elasto-optic model.[2] The stress-optic model has been studied e.g., in the references.[9,12–15]

4.1 *Stress-optic Coefficients*

Stress-optic model applies the stress-optic coefficients C_1 and C_2 that will be related to the elasto-optic coefficients in Eq. (28). By using the coefficients C_1 and C_2, we can calculate the radial, tangential and axial components of the stress-induced index change in the fiber core. The three refractive index components calculated with the stress-optic coefficients are[9]

$$n_r(x) = n(x) - C_1(x)\sigma_r(x) - C_2(x)[\sigma_\theta(x) + \sigma_z(x)], \tag{21}$$

$$n_\theta(x) = n(x) - C_1(x)\sigma_\theta(x) - C_2(x)[\sigma_r(x) + \sigma_z(x)], \tag{22}$$

$$n_z(x) = n(x) - C_1(x)\sigma_z(x) - C_2(x)[\sigma_r(x) + \sigma_\theta(x)], \tag{23}$$

where $\sigma_r(x), \sigma_\theta(x), \sigma_z(x)$ are the radial, tangential, and axial stresses as a function of the radial position x. $n(x)$ is the refractive index of unstressed glass at a radial position x.

We will assume that bending of a fiber will cause only axial stress so that $\sigma_\theta = 0$ and $\sigma_r = 0$. Using these values in Eq. (21), we can calculate the radial refractive index change n_r for the linearly polarized mode LP_{01}

$$\Delta n_r = n_r - n = -C_2\sigma_z. \tag{24}$$

When modeling higher-order optical modes that have tangential or axial field components, one will also need the other stress-induced index change components Δn_θ and Δn_z of a bent fiber

$$\Delta n_\theta = -C_2\sigma_z, \quad \Delta n_z = -C_1\sigma_z.$$

The values of C_1 and C_2 in SiO_2 glass with refractive index n are[5]

$$C_1 = \frac{n^3}{2} \cdot 4.4710^{-7}/\text{MPa} = 0.688 \cdot 10^{-6}/\text{MPa}$$

and

$$C_2 = \frac{n^3}{2} \cdot 2.836 \cdot 10^{-6}/\text{MPa} = 4.39 \cdot 10^{-6}/\text{MPa}.$$

In some sources C_1 and C_2 values have not been multiplied with $n^3/2$, but instead $n^3/2$ is included in the formulas of refractive index changes.

4.2 *Relations between Elasto-Optic and Stress-Optic Coefficients*

Applying Hooke's law,[16] $\sigma_z(x) = E(x)(\frac{\Delta s(x)}{s})$, in a bent fiber we can calculate the elastic modulus $E(x)$:[17]

$$E(x) = \frac{\sigma_z(x)}{(\frac{\Delta s(x)}{s})} = \frac{\sigma_z(x)}{(\frac{2\pi x\alpha}{2\pi R\alpha})} = \frac{\sigma_z(x)}{(\frac{x}{R})}, \tag{25}$$

where α is the bending angle, $\Delta s(x)$ is the change of the length due to bending of the fiber, s is length of the bent fiber, x is the radial distance from the center of the fiber, $\sigma_z(x)$ is the local axial bending stress, and R is the radius of curvature of the fiber.

It is useful to have a conversion between the elasto-optic and stress-optic coefficients. We can define matrix elements s_{11} and s_{12}[18]

$$s_{11} = \frac{1}{E}, \quad s_{12} = -\frac{v}{E}.$$

The relations between the elasto-optic (p_{11}, p_{12}) and stress-optic coefficients (C_1, C_2) are given in Refs. 9 and 18:

$$C_1 = \frac{n^3}{2}(s_{11}p_{11} + 2s_{12}p_{12}), \tag{26}$$

$$C_2 = \frac{n^3}{2}[s_{11}p_{12} + s_{12}(p_{11} + p_{12})], \tag{27}$$

where n is a refractive index of an unstressed material at a given wavelength.

Using Eqs. (26) and (27) and the elasto-optic values given in Ref. 5, $p_{11} = 0.121$ and $p_{12} = 0.270$, we can calculate the stress-optic coefficients C_1 and C_2 in a silica fiber

$$\begin{aligned} C_1 &= \frac{n^3}{2E}(p_{11} - 2vp_{12}) = 0.688 \cdot 10^{-6}/\text{MPa} \\ C_2 &= \frac{n^3}{2E}(p_{12} - v(p_{11} + p_{12})) = 4.388 \cdot 10^{-6}/\text{MPa}. \end{aligned} \tag{28}$$

When elasto-optic and stress-optic coefficient values are related by Eq. (28), the two models will give identical values for the stress-induced index changes. We will use the C_1 and C_2 values given in Eq. (28) in the stress-optic model for undoped SiO_2.

Similarly, we can also solve the elasto-optic coefficients p_{11} and p_{12} using the stress-optic coefficients C_1 and C_2 from Eqs. (26) and (27).

$$p_{11} = \frac{2}{n^3}\frac{(s_{11}+s_{12})C_1 - 2s_{12}C_2}{(s_{11}+2s_{12})(s_{11}-s_{12})}, \tag{29}$$

$$p_{12} = \frac{2}{n^3}\frac{s_{11}C_2 - s_{12}C_1}{(s_{11}+2s_{12})(s_{11}-s_{12})}. \tag{30}$$

5 Bending Stress Induced Refractive Index Changes in the Stress-optic Model

With the stress-optic coefficient value $C_2 = 4.388 \cdot 10^{-6}/\text{MPa}$ and the elastic modulus value $E = 72.6$ GPa of SiO_2, we can calculate the bending induced refractive index change $\Delta n_{SO}(x)$ using Eqs. (24)–(32). Equation (24) gives the radial refractive index change

$$\Delta n_{SO}(x) = \Delta n_r(x) = -C_2(x)\sigma_z(x). \tag{31}$$

From the elastic modulus [Eq. (25)], we can solve the bending induced axial stress at a radial position x

$$\sigma_z(x) = \frac{x}{R}E(x). \tag{32}$$

Then, the stress induced refractive index change in Eq. (31) is

$$\Delta n_{SO}(x) = -C_2(x)E(x)\left(\frac{x}{R}\right). \tag{33}$$

The refractive index $n_{SO}(x)$, by the stress-optic model, at a radial position x, including the stress-induced index change $\Delta n_{SO}(x)$, is

$$\begin{aligned} n_{SO}(x) &= n(x) + \Delta n_{SO}(x) \\ &= n(x) - C_2(x)E(x)\left(\frac{x}{R}\right). \end{aligned} \tag{34}$$

The refractive index profile $n_{SO}(x)$ in the stress-optic model without conformal transformation, is

$$n_{SO}(x) = \left[1 - \frac{C_2 E}{n(x)}\left(\frac{x}{R}\right)\right]n(x), \tag{35}$$

where $n(x)$ is the original index profile of an unstressed fiber.

Using the values of undoped silica, $E_{SiO2} = 72.6$ GPa and $C_2 = 4.388 \cdot 10^{-6}/\text{MPa}$,[5] we will have $\frac{C_2 E}{n} = 0.2186$. The stress-optic model result $n_{SO}(x)$ in Eq. (35) can be compared to the result $n_{EO}(x)$ of the elasto-optic model given in Eq. (10). Due to the relations Eqs. (26) and (27) between the elasto-optic and stress-optic coefficients, the multipliers of the term (x/R) in Eqs. (8) and (35) have equal values.

5.1 *Conformal Transformation of Refractive Index Profiles in the Stress-Optic Model*

A conformal transformation given in Eq. (5) can be applied to the bending stress induced refractive index profile $n_{SO}(x)$ that is given in Eq. (34). This transformation will give a refractive index profile $n_{CSO}(x)$ of a curved waveguide including bending stress-induced index changes

$$n_{\mathrm{CSO}}(x) = \left(1 + \frac{x}{R}\right)\left[n(x) - C_2(x)E(x)\left(\frac{x}{R}\right)\right]$$
$$= n(x) - C_2(x)E(x)\left(\frac{x}{R}\right) + \left(\frac{x}{R}\right)n(x) - C_2(x)E(x)\left(\frac{x}{R}\right)^2. \quad (36)$$

Removing the small, second-order term $-C_2E(\frac{x}{R})^2$, we will have

$$n_{\mathrm{CSO}}(x, R) = \left(1 + \frac{n(x) - C_2(x)E(x)}{n(x)}\left(\frac{x}{R}\right)\right)n(x). \quad (37)$$

If the necessary data is available, we should use mixed $C_{2\mathrm{mix}}(x)$ values given in Eq. (43), for doped cores and substitute the elastic modulus value $E(x)$ in Eq. (37) with the $E_{\mathrm{mix}}(x)$ given in Eq. (43) to model the doping effects.

5.2 *Effective Bending Radius of Conformally Transformed Stress-Optic Index Profiles*

The conformally transformed stress-optic index profile, $n_{\mathrm{CSO}}(x)$ in Eq. (37), can be written also with the effective bending radius R_{eff}, as

$$n_{\mathrm{CSO}}(x, R) = \left(1 + \frac{x}{R_{\mathrm{eff}}}\right)n(x), \quad (38)$$

where

$$R_{\mathrm{eff}} = \frac{n(x)}{n(x) - C_2E}R. \quad (39)$$

If we use $C_2 = 4.388 \cdot 10^{-6}/\mathrm{MPa}$ and $E = 72.6$ GPa of undoped SiO_2 glass, then $C_2E = 0.31854$. By approximating $n(x) = 1.4572$ in Eq. (39), we can calculate an effective bending radius R_{eff}, in the conformally transformed stress-optic refractive index model CSO, as

$$R_{\mathrm{eff}} \approx \frac{1.4572}{1.4572 - 0.31854}R = 1.280R. \quad (40)$$

Thus, the conformally transformed stress-optic index profile $n_{\mathrm{CSO}}(x, R)$ in Eq. (38), without doping effects, is

$$n_{\mathrm{CSO}}(x, R) = \left(1 + \frac{x}{1.280R}\right)n(x). \quad (41)$$

We can compare Eq. (41), given by the conformally transformed stress-optic model with Eq. (20) given by the conformally transformed elasto-optic model, where $n_{\mathrm{CEO}}(x) = (1 + \frac{x}{1.280R})n(x)$. The effective bending radius values are equal, as expected: $R_{\mathrm{eff}} = 1.280R$ in the CEO model and in the CSO model.

5.3 *Effective Bending Radius in the Elasto-optic and Stress-optic Models*

The refractive index profile and effective bending radius equations in the elasto-optic and stress-optic models are summarized in Table 2.

An effective bending radius R_{eff} of a fiber does not depend on the stress model we will use. Equation (39) for effective bending radius $R_{\mathrm{eff,CSO}}$, which was derived using the stress-optic model, is equal to Eq. (18) for $R_{\mathrm{eff,CEO}}$ derived using the elasto-optic model. This can be seen easily

Table 2 Conformally transformed refractive index profiles $n_{\mathrm{CEO}}(x, R)$ from Eq. (12) in the elasto-optic model and $n_{\mathrm{CSO}}(x, R)$ from Eq. (37) in the stress-optic model.

Model	Refractive index profile	Effective bending radius
Stress-optic	$n_{\mathrm{CSO}}(x, R) = (1 + \frac{n(x) - C_2(x)E(x)}{n(x)}(\frac{x}{R}))n(x)$	$R_{\mathrm{eff}} = \frac{n}{n - C_2 E} R$
Elasto-optic	$n_{\mathrm{CEO}}(x, R) = (1 + \frac{x}{R})[n(x) - \frac{n^2}{2}(p_{12} - v(p_{11} + p_{12}))(\frac{x}{R})n(x)]$	$R_{\mathrm{eff}} = \frac{R}{[1 - \frac{n^2}{2}(p_{12} - v(p_{11} + p_{12}))]}$

$$R_{\mathrm{eff,CSO}} = \frac{n}{n - C_2 E} R = \frac{n}{n\left(1 - \frac{1}{n} C_2 E\right)} R = \frac{1}{1 - \frac{n^3}{2n}(p_{12} - v(p_{11} + p_{12}))} R$$
$$= \frac{1}{1 - \frac{n^2}{2}(p_{12} - v(p_{11} + p_{12}))} R = R_{\mathrm{eff,CEO}}, \tag{42}$$

where $C_2 E$ was solved from Eq. (28).

6 Defining Material Constants *E* and C_2 of Doped SiO_2 Glass

6.1 *Measuring Stress-optic Coefficient $C_2(x)$ in a Bent Optical Fiber*

The values of the elastic modulus $E(x)$ and stress-optic coefficient $C_2(x)$ depend on the doping concentrations. They can be calculated for the doped SiO_2 glass using the E_{mix} and $C_{2\mathrm{mix}}$ values[13]

$$E_{\mathrm{mix}}(x) = \Sigma_i^n a_i(x) E_i(x) \tag{43}$$

$$C_{2\mathrm{mix}}(x) = \Sigma_i^n a_i(x) C_{2i}(x),$$

where $a_i(x)$ are the (vol%) concentrations of the dopant materials, $E_i(x)$ are the elastic modulus values of the pure dopant materials, and $C_{2i}(x)$ are the stress-optic coefficient values of the pure dopant materials. n is the number of different materials in the glass.

If we can measure the value $\Delta n_{\mathrm{SO}}(x)$ in Eq. (33), and if we know the $E_{\mathrm{mix}}(x)$ of the glass, we can estimate the values of $C_{2\mathrm{mix}}(x)$ in a doped glass solving Eq. (33) without knowing the C_{2i} values of pure dopant materials

$$C_{2\mathrm{mix}}(x) = -\frac{R}{x}\frac{\Delta n_{\mathrm{SO}}(x)}{E_{\mathrm{mix}}(x)}. \tag{44}$$

The relation in Eq. (44) allows us to find out the stress-optic coefficient values $C_{2\mathrm{mix}}(x)$ if we can measure the bending stress-induced index change $\Delta n_{\mathrm{SO}}(x, R)$ of a fiber and calculate the $E_{\mathrm{mix}}(x)$ values of the same fiber.

This method works better with large values of x. Calculated $C_{2\mathrm{mix}}(x)$ results have high variation near the center of the fiber where x-coordinate approaches zero.

If we know the elastic modulus E_i and stress-optic values C_{2i} of the dopant materials (see Table 3) and the dopant concentrations in the SiO_2 glass, we can calculate the mixed elastic modulus value E_{mix} and mixed stress-optic coefficient $C_{2\mathrm{mix}}$ of doped silica using Eqs. (43). However, there exist differences between the published E_i and C_{2_i} values.

7 Stress Induced Refractive Index Profiles of Bent Optical Fibers

7.1 *Measured and Modelled Index Profiles of Bent Fibers*

We measured refractive index profiles $\Delta n(x)$ of straight fibers and profiles $\Delta n'(x)$ of the same fibers when they were bent (see Figs. 4 and 5). The measurement was done with an IFA-100 profiler in straight and bent optical fibers. The measured refractive index profiles of the bent fibers include stress induced refractive index changes, but not the virtual refractive index changes, that the light experiences when it travels in curved optical fibers.

We adjusted the combined $C_{2\mathrm{mix}}(x)E_{\mathrm{mix}}(x)$ values when simulating the bending stress-induced index profiles using Eq. (37). The $C_{2\mathrm{mix}}(x)E_{\mathrm{mix}}(x)$ values were selected so that the simulated stress-optic index profiles $n_{\mathrm{CSO}}(x,R)$ matched with the measured index profiles of bent fibers.

Figure 5 shows matched refractive index profiles of an Al_2O_3 doped fiber.

If we know the glass material composition, we can calculate the elastic modulus $E_{\mathrm{mix}}(x)$ values. Then we can estimate the values of the stress-optic coefficients $C_{2\mathrm{mix}}(x)$ from the measured bent fiber index profile $\Delta n_{\mathrm{SO}}(x)$ using Eq. (44).

The value of the effective bending radius R_{eff} in Eq. (39) can be calculated if we can calculate or measure the combined $C_{2\mathrm{mix}}(x)E_{\mathrm{mix}}(x)$ values. The $C_{2\mathrm{mix}}(x)E_{\mathrm{mix}}(x)$ values can be studied experimentally by matching the modeled stress-induced index profile $n_{\mathrm{SO}}(x,R)$ in Eq. (35) with the measured refractive index profile of a bent fiber. This is done in Figs. 4 and 5.

Table 3 Examples of E, Poisson's ratio ν and C_2 values of some glass materials.

Glass material	Elastic modulus	ν	C_2/MPa^{-1}[a]	References
SiO_2	72.6 GPa	0.164	$4.39 \cdot 10^{-6}$	5
Al_2O_3	177 GPa	0.25	—	19
Al_2O_3	—	—	$0.37 \cdot 10^{-6}$	20
GeO_2	45.0 GPa	0.212	$6.86 \cdot 10^{-6}$	20

[a]C_2 values are calculated using Eq. (28) and ν, p_{11}, and p_{12} values given in Refs. 5 and 20.

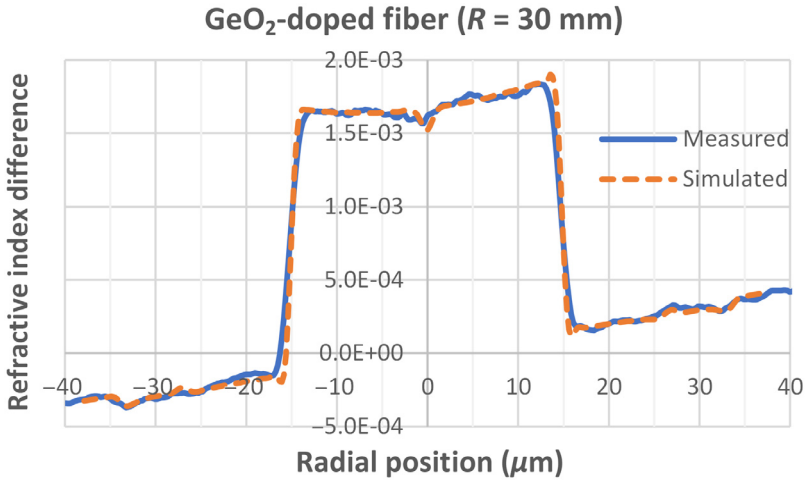

Fig. 4 Simulated (with $C_2E = 0.232$ in the core and $C_2E = 0.295$ in the cladding) and measured stress induced refractive index profiles of a GeO_2 doped bent fiber (bending $R = 30$ mm).

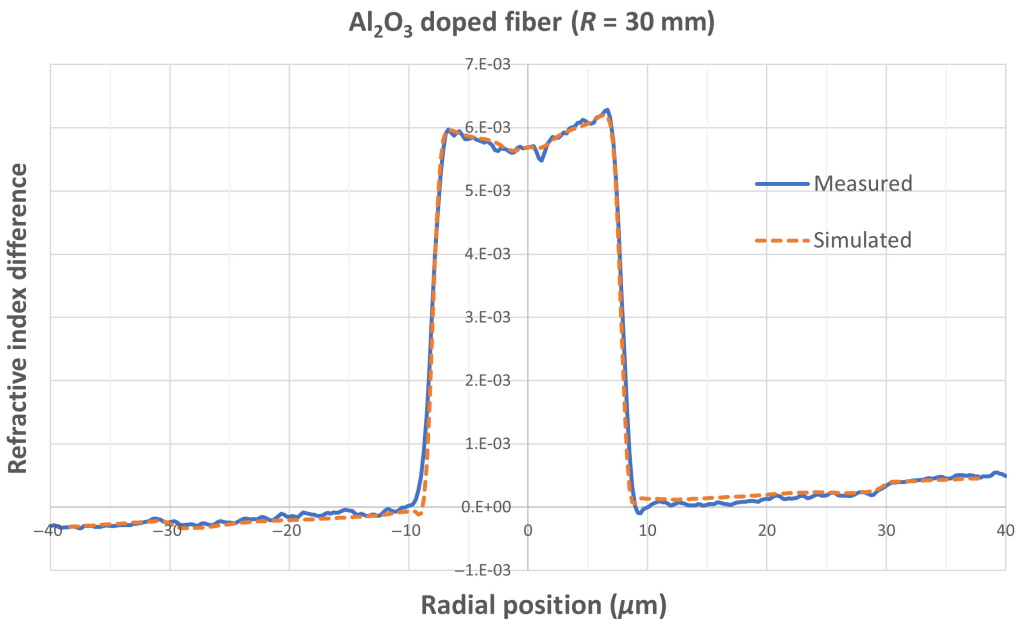

Fig. 5 Simulated (with $C_2E = 0.56$ in the core and $C_2E = 0.302$ in the cladding) and measured stress induced refractive index profiles of an Al_2O_3 doped bent fiber (bending $R = 30$ mm).

7.2 *Estimating Stress-Optic Coefficients* C_2

Elastic modulus depends only on doping materials, and $E_{\text{mix}}(x)$ can be calculated using known or measured glass material composition data. Thus $C_{2\text{mix}}(x)$ can be solved if the radial $\Delta n_{\text{straight}}(x)$ and $\Delta n_{\text{bent}}(x)$ values in the equation

$$C_{2\text{mix}}(x)E_{\text{mix}}(x) = \frac{R}{x}[\Delta n_{\text{straight}}(x) - \Delta n_{\text{bent}}(x)],$$

can be measured accurately enough.

We can estimate the $C_{2\text{mix}}(x)E_{\text{mix}}(x)$ values by minimizing the value of the difference between the measured and modeled refractive index profiles. The $C_{2\text{mix}}(x)E_{\text{mix}}(x)$ are the values that minimize the difference:

$$\int_a^b (n_{\text{meas}}(x) - n_{\text{mod}}(x))^2 \mathrm{d}x,$$

where a and b define the radial distance where the dopant concentration is constant.

We studied $C_2(x)$ values of SiO_2 in the cladding area of 16 fibers with different geometries. This study gave a value $C_2 = (4.5 \pm 0.8)10^{-6}/\text{MPa}$. The average value is near the C_2 value given for SiO_2 in Table 3, but it has large uncertainty. In the core area the analyzed $C_{2\text{mix}}(x)$ values had even higher variation. It will be necessary to improve the bent fiber measurement technique to decrease the variation especially in the core area.

7.3 *Challenges to Define* C_{2i} *Values*

The applied refractive index measurement device is not designed to measure bent fiber refractive index profiles. The refractive index measurement accuracy near the center of a bent fiber was not good enough. Since the analyzed doped areas were near the center of the fiber, the $C_{2\text{mix}}(x)$ values in that area had high variation. Also, low dopant material concentrations decrease the accuracy of defining C_{2i} values of the individual dopant materials.

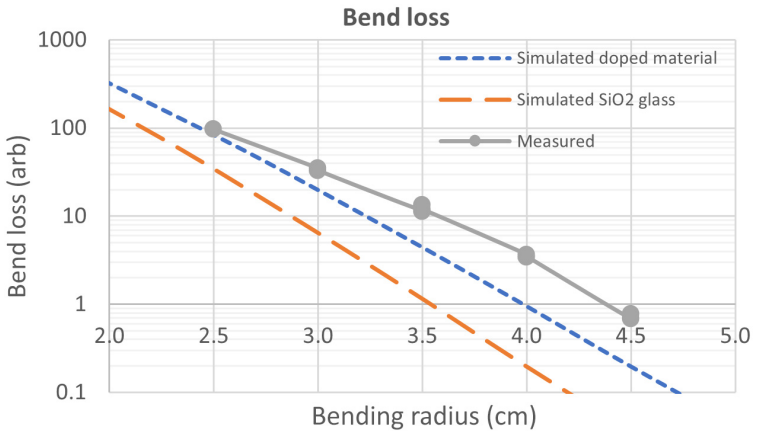

Fig. 6 Measured bend loss values compared to two simulated bend loss curves of a large mode area fiber.

8 Simulated and Measured LP_{01} Bend Loss Values

Figure 6 shows two simulated and one measured bend loss curve of an active fiber as a function of a bending radius. We transformed conformally a refractive index profile of that fiber including bending stresses but without dopant material contribution. That index profile was used in bend loss simulations. Another bend loss simulation was done with the index profile of the same fiber, but this time with the bending stresses that were modified by dopant materials using $C_{2\text{mix}}$ and E_{mix} values.

The simulated values are closer to the measured values when the doping materials are included in the stress model.

It is possible to improve bend loss simulations by using a virtual refractive index profile including stress effects based on dopant materials instead of simulating a refractive index profile with stress effects based on an undoped SiO_2 fiber.

9 Summary

We calculated refractive index profiles of bent optical fibers using elasto-optic and stress-optic models. These two models are mathematically equal. In the bent fiber simulations, we applied a more accurate refractive index model that combines conformal transformation of a curved waveguide with bending stress-induced index changes of doped glass. Using known or measured dopant material concentrations or using measured refractive index profiles of bent fibers we can improve our bend loss estimations.

10 Conclusions

We applied elasto-optic and stress-optic models to estimate refractive index changes in bent optical fibers. We derived formulas for conformally transformed elasto-optic and stress-optic refractive index profiles for bent optical fibers. They are given in Eqs. (14) and (36) and in Table 2. The two models are equal when the material coefficients are calculated using the same input data. Conformal mapping of the index profile is an effective method to analyze a curved circular waveguide and it enables a simple way of combining the bending stress effects with the input data.

In the simulations, one can use a linear mixture of the published C_2 and E values for estimating the $C_{2\text{mix}}$ and E_{mix} values of the doped glass materials. When the doping materials are included in the stress models, simulated bend loss values are closer to the measured values. More accurate input data improves the simulation results independent of the method that is used to solve the Maxwell equations.

Acknowledgments

We would like to acknowledge the personnel of nLight Inc. for making and testing the fibers and MA. H. Ukonmaanaho and Ms. T. Kiiveri for kindly reading and commenting this article. Ms. S. Kiiveri is acknowledged for drawing Fig. 1. This article is based on our work presented at the Photonics West 2022 conference.[17]

References

1. M. Heiblum and J. H. Harris, "Analysis of curved optical waveguides by conformal transformation," *IEEE J. Quantum Electron.* **11**(2), 75–83 (1975).
2. R. T. Schermer and J. H. Cole, "Improved bend loss formula verified for optical fiber by simulation and experiment," *IEEE J. Quantum Electron.* **43**(10), 899–909 (2007).
3. D. Marcuse, "Field deformation and loss caused by curvature of optical fibers," *J. Opt. Soc. Am.* **66**(4), 311–320 (1976).
4. B. Frey et al., "Semicomputational calculation of Bragg shift in stratified materials," *Phys. Rev. E* **104**, 055307 (2021)
5. M. Bass, *Handbook of Optics, Vol. II, Devices, Measurements and Properties*, Chapter 33, Properties of crystals and glasses, McGraw-Hill, New York (1995).
6. G. A. Rosales-Sosa, A. Masuno, and H. Inoue, "Crack-resistant Al_2O_3–SiO_2 glasses," *Sci. Rep.* **6**, 23620 (2016).
7. Heraeus, "Properties of fused silica," (2022). https://www.heraeus.com/en/hca/fused_silica_quartz_knowledge_base_1/properties_1/properties_hca.html (accessed 3 August 2022).
8. L. A. Sánchez et al., "High accuracy measurement of Poisson's ratio of optical fibers and its temperature dependence using forward-stimulated Brillouin scattering," *Opt. Express* **30**(1), 42–52 (2022).
9. G. W. Scherer, "Stress-induced index profile distortion in optical waveguides," *Appl. Opt.* **19**(12), 2000–2006 (1980).
10. W. Sellmeier, "Zur Erklärung der abnormen Farbenfolge im Spectrum einiger Substanzen," *Ann. Phys. Chem.* **219**(6), 272 (1871).
11. P. Kiiveri, *Design, Fabrication and Characterization of Optical Fibers for Amplifiers, Telecommunications and Sensors*, University of Technology, Dept. for Electrical Communications Engineering, Helsinki (1999).
12. P. Kiiveri et al., "Stress induced refractive index changes in preforms and laser fibers," *Proc. SPIE* **10897**, 1089727 (2019).
13. P. Kiiveri et al., "Stress-induced refractive index changes in laser fibers and preforms," *IEEE Photonics J.* **11**(6), 1–10 (2019).
14. W. Primak and D. Post, "Photoelastic constants of vitreous silica and its elastic coefficient of refractive index," *J. Appl. Phys.* **30**(5), 779 (1959).
15. D. Brickus and A. Dementjev, "On the use of photoelastic effect and plane strain or plane stress approximations for the description of thermal lensing," *Lith. J. Phys.* **56**, pp. 9–20 (2016).
16. D. E. Roller and R. Blum, *Physics: Mechanics, Waves, and Thermodynamics*, p. 360, Holden-Day Inc. (1981).
17. P. Kiiveri et al., "Refractive index profiles and propagation losses in bent laser fibers," *Proc. SPIE* **11981**, 1198118 (2022).
18. D. C. Brown and H. J. Hoffman, "Thermal stress and thermo-optic effects in high average power double-clad silica fiber lasers," *IEEE J. Quantum Electron.* **37**(2), 207–217 (2001).
19. V. Rontu et al., "Elastic and fracture properties of free-standing amorphous ALD Al2O3 thin films measured with bulge test," *Mater. Res. Exp.* **5**(4), 046411 (2018).
20. P. D. Dragic et al., "A unified materials approach to mitigating optical nonlinearities in optical fiber. II. B. The optical fiber, material additivity and the nonlinear coefficients," *Int. J. Appl. Glass Sci.* **9**, 307–318 (2018).

Biographies of the authors are not available.